# Methane Hydroxylation on a Diiron Model of Soluble Methane Monooxygenase#

**Kazunari Yoshizawa,* Takehiro Ohta, and Tokio Yamabe†**

Department of Molecular Engineering, Kyoto University, Sakyo-ku, Kyoto 606-8501

†Institute for Fundamental Chemistry, 34-4 Takano-Nishihiraki-cho, Sakyo-ku, Kyoto 606-8103

(Received February 12, 1998)

A concerted mechanism is proposed for the conversion of methane to methanol on intermediate **Q** of soluble methane monooxygenase (sMMO), the active species of which is considered to involve an $Fe_2(\mu\text{-}O)_2$ diamond core. A hybrid density functional theory (DFT) method is used. Methane is highly activated on the dinuclear iron complex through the formation of the **Q**($CH_4$) complex, in which a four-coordinate iron plays a central role in the bonding interactions between intermediate **Q** and methane. An H atom abstraction via a four-centered transition state and a methyl migration via a three-centered transition state successively occur within the complex, leading to the formation of product methanol. The reaction pathway for the methane hydroxylation on the diiron complex follows the mechanism for the gas-phase reaction by the bare $FeO^+$ complex described in a previous paper (K. Yoshizawa, Y. Shiota, and T. Yamabe, *Chem. Eur. J.*, **3**, 1160 (1997)). Our mechanism for the methane hydroxylation by sMMO is against a radical mechanism which has been widely believed to play a role in hydrocarbon hydroxylations by cytochrome P450.

Activation of methane[1—9] has attracted increased attention in recent years because of its scientific and industrial importance. In particular, methanol prepared from methane is of great interest as an important energy source in the coming twenty-first century. A commercial process for the production of methanol from natural gas which mainly consists of methane involves two-step reactions, (1) and (2), via the formation of synthesis gas, i.e., carbon monoxide and dihydrogen.[5,6] The Fischer–Tropsch reaction converts synthesis gas into a mixture of long-chain alkanes and alcohols, important fuels for internal-combustion engine and thermal power generation.

$$CH_4(g) + H_2O(g) \longrightarrow CO(g) + 3H_2(g) \quad (1)$$
$$\Delta H^\circ = 49.3 \text{ kcal mol}^{-1}$$

$$CO(g) + 2H_2(g) \longrightarrow CH_3OH(g) \quad (2)$$
$$\Delta H^\circ = -21.7 \text{ kcal mol}^{-1}$$

Direct conversion of methane to methanol, indicated in reaction (3), is an energetically favorable process compared with the available commercial one, and thus it is of intense current interest in pure and applied chemistry.

$$CH_4(g) + 1/2O_2(g) \longrightarrow CH_3OH(l) \quad (3)$$
$$\Delta H^\circ = -30.7 \text{ kcal mol}^{-1}$$

Methane monooxygenase (MMO),[10] which exists in some methanotrophs as an iron-containing soluble form and a copper-containing membrane form, catalyzes the direct methane hydroxylation efficiently under physiological conditions. This enzyme greatly contributes to the preservation of the environment through limiting the release of methane into the atmosphere, because this greenhouse gas is produced in enormous quantities in the environment as the primary product of anaerobic metabolism by methanogenic bacteria. Structural analyses of various intermediates of soluble MMO (sMMO) have been extensively performed. The key intermediate **Q** of sMMO, the species responsible for direct reactivity toward methane, has been proposed to involve a high-valent dinuclear Fe(IV) complex.[11] Que, Lipscomb, and their collaborators[12] have recently suggested from Mössbauer and EXAFS analyses that the active site of intermediate **Q** should involve an $Fe_2(\mu\text{-}O)_2$ "diamond" core. Although X-ray structural analyses have not yet been successful for intermediate **Q**, the first coordination sphere around the two iron sites has been proposed to consist of 4.5 O/N on the average.[12]

The gas-phase C–H and C–C bond activation of small hydrocarbons by various transition-metal-oxide ions and bare metal cations have been extensively investigated in Schwarz's[13] and Armentrout's[14] laboratories. Detailed analyses of various gas-phase reactions of methane, higher alkanes, alkenes, benzene, and other compounds with the bare $MO^+$ complexes have been carried out, in which M is a first-row transition metals. The methane–methanol conversion by $FeO^+$ is of great interest, since this process may be viewed as a simple model for catalytic and enzymatic alkane hydroxylation. On the basis of experimentally determined isotope effects, Schröder and Schwarz[13a] have suggested that a reaction species, $HO\text{–}Fe^+\text{–}CH_3$, plays a central role in the

# In memory of Professor Kenichi Fukui, a chemist who increased our understanding of chemical reactions.

reaction between $FeO^+$ and $CH_4$. A similar reaction species, $HO–Co^+–CH_3$, has been also suggested by Armentrout et al.[14j] to play an important role in the gas-phase reaction of methane with $CoO^+$.

On methane and C–H bond activation, there has been a large amount of theoretical work by Saillard and Hoffmann,[15] Goddard et al.,[16] Siegbahn, Blomberg, and their collaborators,[17] Ziegler et al.,[18] Morokuma, Koga, and their collaborators,[19] Sakaki and Ieki,[20] and Cundari.[21] In a recent paper,[22] we have proposed two kinds of reaction pathways for the gas-phase methane–methanol conversion by $FeO^+$ on the basis of Fukui's IRC (intrinsic reaction coordinate)[23] analysis coupled with density functional theory (DFT) calculations. We have shown that the reaction pathway via the hydroxy intermediate ($HO–Fe^+–CH_3$) is energetically more favorable than the other one via the methoxy intermediate ($H–Fe^+–OCH_3$). The favorable reaction pathway we have proposed from detailed computational analyses is indicated in Scheme 1

From extended Hückel as well as DFT calculations,[24–26] we have proposed that the concerted mechanism in Scheme 1 should also play an important role in the enzymatic methane hydroxylation by sMMO. An important difference between the gas-phase and enzymatic reactions is the charge states of the active iron species; the formal charge of the iron active center in the enzymatic reaction is +4 while that in the gas-phase reaction is +3. The C–H bonds of methane are significantly weakened by the formation of the reactant complex, $\mathbf{Q}(CH_4)$, which is weakly bound through Fe–C as well as Fe–H bonds. We have indicated that successively occurring H atom abstraction and methyl migration at the iron active center lead to the final product complex involving methanol as a ligand. Our proposal[22,24–26] argues against a widely accepted radical mechanism for hydrocarbon hydroxylations by cytochrome P450, i.e., the so-called oxygen-rebound mechanism.[27]

Siegbahn and Crabtree[28] recently proposed from DFT calculations that the conversion of methane to methanol on a dinuclear model complex of intermediate **Q** of sMMO should occur in a way similar to the oxygen-rebound mechanism for alkane hydroxylations by cytochrome P450. The first step of the proposed mechanism is a direct H atom abstraction by a ferryl "oxygen" in the dinuclear complex. They have proposed that a linear C–H–O array should occur in the transition state for H atom abstractions by iron-oxo species. The mechanism of Siegbahn and Crabtree[28] and ours[22,24–26] are strikingly different in the early stages concerning H atom abstraction from methane.

In this article, we propose from DFT computations that the conversion of methane to methanol on intermediate **Q** of sMMO should occur reasonably well on the basis of the concerted mechanism (indicated in Scheme 1) for the gas-phase methane hydroxylation by $MnO^+$, $FeO^+$, and $CoO^+$.[22,29] In a previous short paper,[26b] we discussed the first half of our concerted reaction pathway (an H atom abstraction from methane) on a diiron model complex of intermediate **Q** which involves an $Fe_2(\mu\text{-}O)_2$ "diamond" core. One of the two iron centers of the dinuclear model complex is responsible for this important enzymatic reaction. We discuss here the entire reaction pathway for the conversion of methane to methanol in detail.

## Diiron Models and Method of Calculation

Our theoretical models of intermediate **Q** of sMMO are indicated in **1** and **2** (Chart 1). These models contain an $Fe_2(\mu\text{-}O)_2$ diamond core with a $\mu$-carboxylato bridge that is a common feature in the structures of diiron enzymes, following the suggestion by Lipscomb, Que, and their collaborators.[12] From their EXAFS analyses, the first coordination sphere around the two iron sites of **Q** has been proposed to consist of 4.5 O/N on the average, as mentioned. Thus, we set up the two diiron models as follows: **1** in which the two irons are both five-coordinate and **2** in which the two irons are five- and four-coordinate. We used aqua ligands to form the four- and five-coordination environments of the iron centers in these models. The formal charge of each iron is +4, that of the oxo species −2, that of the carboxylato bridge −1, and the water ligands neutral; as a consequence the total charge of each model complex is +3.

The Gaussian 94 program package[30] was used for hybrid (Hartree–Fock/DFT) B3LYP calculations.[31,32] The B3LYP method consists of the Slater exchange, the Hartree–Fock exchange, the exchange functional of Becke,[31] the correlation functional of Lee,

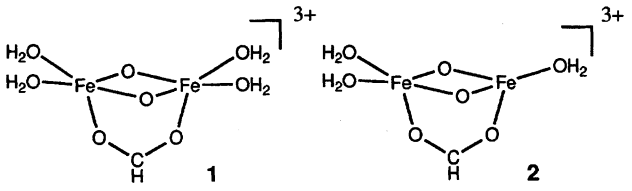


Chart 1.

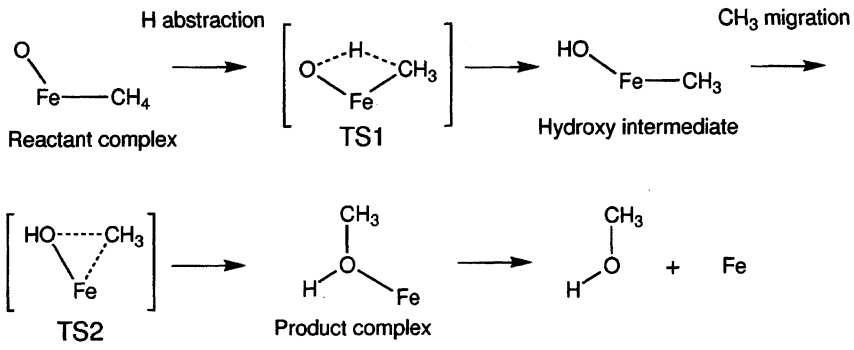


Scheme 1.

Yang, and Parr (LYP),[32] and the correlation functional of Vosco, Wilk, and Nusair.[33] The contribution of each energy to the B3LYP energy expression of Eq. 4 was fitted by Becke[31b] empirically on a reference set of molecules. We used the double-$\zeta$ valence basis set (8s5p5d)/[3s3p2d][34] with the ECP (effective core potential) replacing core electrons up to 2p for the Fe atom, and the standard double$\zeta$ basis sets[35] for the H, C, and O atoms. These basis sets are referred to as LanL2DZ following the basis set code of the Gaussian 94 program. Excellent performance of the B3LYP method combined with effective core potentials was recently reported for iron-containing complexes.[36]

$$E^{\mathrm{B3LYP}}=(1-a_0)E_{\mathrm{x}}^{\mathrm{Slater}}+a_0E_{\mathrm{x}}^{\mathrm{HF}}+a_{\mathrm{x}}E_{\mathrm{x}}^{\mathrm{Becke}}+a_{\mathrm{c}}E_{\mathrm{c}}^{\mathrm{LYP}}+(1-a_{\mathrm{c}})E_{\mathrm{c}}^{\mathrm{VWN}} \quad (4)$$

$$a_0=0.2,\ a_{\mathrm{x}}=0.72,\ a_{\mathrm{c}}=0.81$$

We optimized local minima corresponding to reactant complex, reaction intermediate, and product complex and saddle points corresponding to transition states (TSs) using the B3LYP method. We could not perform systematic vibrational analyses for the large dinuclear systems in spite of our best efforts because the LanL2DZ basis set do not allow analytical evaluation of Hessians. However, essential parts of the optimized geometries are quite similar to those for the gas-phase methane hydroxylation by $FeO^+$ and thus we think that the geometry optimizations were correctly performed.

The spin states of **1** and **2** were set to be singlet, following the Mössbauer observation by Lipscomb and collaborators.[11] Accordingly, we used the spin-restricted version of the B3LYP method for geometry optimizations to have a first insight concerning the reaction pathway. Clearly, this restriction is theoretically not sufficient since antiferromagnetic coupling between the two Fe(IV) species (with $S=2$ or 1) is appropriate for the observed singlet state of intermediate **Q**. However, we do not think that the essential geometrical features of reaction species along the reaction pathway are spoiled by this methodological shortcoming.[37]

In order to have a better understanding of the reaction pathway, further spin-unrestricted calculations were carried out to refine the potential energy surface from spin-restricted calculations. We attempted to obtain broken-symmetry singlet states in which the two Fe(IV) species are antiferromagnetically coupled. However, it was impossible to obtain such broken-symmetry solutions within the framework of the present DFT method, in spite of our best efforts. We therefore performed spin-unrestricted calculations in the nonet states in which two quintet Fe(IV) species are ferromagnetically coupled. Since Siegbahn and Crabtree[28] also adopted this spin state for their DFT calculations at the same level of theory, the contrast between the two reaction mechanisms will become clear. The local environment at each iron center in the nonet state is essentially the same as that in the antiferromagnetically coupled high-spin Fe(IV) species, while in the nonet state they are ferromagnetically coupled between the two irons. Since one iron center in the dinuclear complex plays an essential role in the methane hydroxylation in our reaction mechanism, we think that calculations under the constraint of the nonet state would not lead to significant erroneous conclusions. Computed $\langle S^2\rangle$ values before annihilation of spin contamination lie in a range of 20.1 —20.4 and they are close to 20.0 after annihilation, the exact value for a nonet state being 20, so that the spin contamination included in spin-unrestricted calculations is negligibly small. In order to have a better insight into this important enzymatic reaction, orbital interaction analyses were performed using the extended Hückel method,[38] implemented with the YAeMOP program package.[39] This approximate molecular orbital method describes general orbital energy trends, major charge shifts, and orbital interactions reasonably well.

## Energetics for the Methane Hydroxylation on a Diiron Complex

The most important stage in our concerted mechanism is an encounter of intermediate **Q** and substrate; one of the "iron" active centers of intermediate **Q** and methane come into contact to lead to the formation of the **Q**($CH_4$) complex. This is strikingly different from a conventional radical mechanism that assumes a linear C–H–O array in its transition state. We found from detailed DFT computations that methane can be bound to a four-coordinate iron, but not to a five-coordinate iron. Thus, model **2** that involves five- and four-coordinate irons is more adequate for our concerted reaction mechanism than model **1** that involves two five-coordinate irons. This computational result may have a relevance to the proposed structure of intermediate **Q**, in which the average coordination number around each iron center has been suggested from EXAFS analyses to be 4.5.[12] Methane is significantly activated through the complex formation; note that the methane in this complex is five-coordinate if we take an Fe–C bond into account.[24b]

A potential energy diagram (from spin-restricted calculations) for the methane–methanol conversion on model **2** is shown in Fig. 1. Essential parts for the optimized structures of the reaction species on the potential energy surface are also illustrated in this diagram, in which water ligands are not present, but exist in actual DFT computations. The reaction pathway is essentially identical to the one we indicated in Scheme 1. At first sight, the potential energy surface in Fig. 1 is downhill toward the product complex, so that we expect the direct methane hydroxylation to occur quite smoothly on this dinuclear complex.

Let us next look at the energetics of the reaction pathway. The binding energy for the **2**($CH_4$) complex was computed to be 27.3 kcal mol$^{-1}$, which is roughly consistent with 22.8 and 22.2 kcal mol$^{-1}$ for the $OFe^+(CH_4)$ complex in the ground sextet state and the low-lying excited quartet state, respectively.[29] Although the binding energy depends on the total charge of the complexes, the bonding occurs in similar manners in $OFe^{2+}(CH_4)$, $OFe^+(CH_4)$, and $OFe(CH_4)$.[40] The bonding in the **2**($CH_4$) complex is slightly affected by a charge-induced dipole effect, but it is mainly due to a direct consequence of the formation of Fe–C as well as Fe–H bonds through important orbital interactions. The methane C–H bonds are significantly activated on the complex through the orbital interactions between the d-block orbitals of the dinuclear complex and the HOMO of methane, as indicated by interaction ① in the diagram of Saillard and Hoffmann (Scheme 2).[41] The unoccupied nonbonding d-block orbital originates from a coordinatively unsaturated iron, i.e., the four-coordinate iron in the model complex **2**. Since the LUMO of methane is high-lying compared with the d-block orbitals, interaction ① is more dominant than interaction ② in activating methane C–H bonds.[24b] In fact, the calculated total charge of the methane in the reactant complex, **2**($CH_4$), is +0.47, due to the significant orbital in-

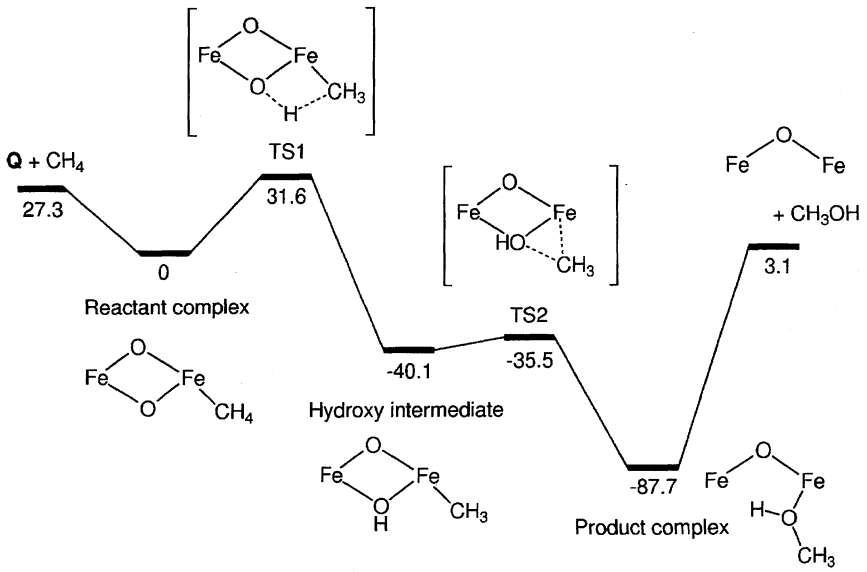


Fig. 1. A potential energy diagram (from restricted B3LYP/LanL2DZ calculations in the singlet state) for the conversion of methane to methanol on a model of intermediate **Q** of sMMO.

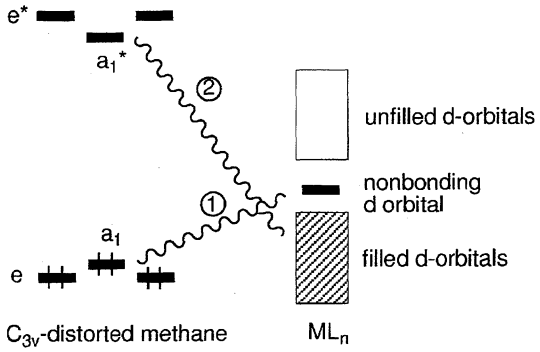


Scheme 2.

teraction ① as well as the charge-induced effect. After that a concerted H atom abstraction occurs at one of the iron centers via the four-centered transition state (TS1) to lead to the hydroxy intermediate, as shown in the illustration in Fig. 1. The activation barrier was calculated to be 31.6 kcal mol$^{-1}$ from spin-restricted B3LYP calculations.

The hydroxy intermediate thus formed is then converted into the product complex via the three-centered transition state (TS2), as indicated in Fig. 1. The activation barrier for TS2 was computed to be only 4.6 kcal mol and we therefore expect that the methyl migration should occur quite easily to lead to the product complex that includes methanol as a ligand. Since this intermediate is extremely stable, nearly 90 kcal mol$^{-1}$ is necessary to liberate the product methanol from the dinuclear complex. This result would partly arise from our model setting. The charge-induced complexation in the product complex would not allow a fragmentation into tricationic and neutral species; we think that it should prefer a dissociation into dicationic and monocationic species. The liberation of neutral methanol is thus overestimated in our model with plus three charge, but we know that the fundamental reaction pathway is independent of the total charge of the complexes.[40] The overall reaction for the formation of methanol was computed to be 24.2 kcal mol$^{-1}$ exothermic.

A potential energy diagram refined by using the spin-unrestricted method is shown in Fig. 2. The general profile of this diagram is probably better than that from spin-restricted calculations shown in Fig. 1. The important energy barrier for TS1 was calculated to be 18.1 kcal mol$^{-1}$ which is smaller than 31.6 kcal mol$^{-1}$ value from spin-restricted calculations. The activation energy for TS2 is 8.4 kcal mol$^{-1}$, being comparable to the value of 4.6 kcal mol$^{-1}$ from spin-restricted calculations. Nearly 65 kcal mol$^{-1}$ is necessary for the liberation of the methanol from the product complex. Although this value is significantly improved from 90 kcal mol$^{-1}$ (the value obtained from spin-restricted calculations in Fig. 1), it is still large. For the gas-phase reaction by $FeO^+$, we also obtained a high liberation energy of 58.6 kcal mol$^{-1}$ in the sextet state.[29] This value is roughly consistent with 65 kcal mol$^{-1}$; much energy is required for the liberation of the methanol from the product complex.

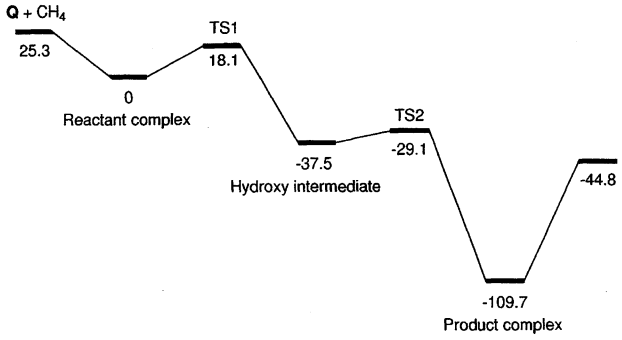


Fig. 2. A potential energy diagram (from unrestricted B3LYP/LanL2DZ calculations in the nonet state) for the conversion of methane to methanol on a model of intermediate **Q** of sMMO.

### Mechanism for the Methane Hydroxylation on a Diiron Complex

Having discussed the potential energy profiles, let us next consider the reaction mechanism in detail by looking at the structures of the reaction intermediates and the transition states. Figure 3 illustrates structures of the reaction species responsible for the intramolecular H atom abstraction on the model complex of intermediate **Q** of sMMO; model complex **2**, the initially formed **2**($CH_4$) complex, TS1, and the hydroxy intermediate. These structures were optimized using the spin-restricted B3LYP method.

In the diamond core of model complex **2**, a couple of Fe–O is long and another couple is short, which is consistent with the head-to-tail dimer of Fe(IV)=O units proposed for the actual intermediate **Q**, as indicated in structure **3** (Chart 2). The computed Fe···Fe distance is 2.78 Å, being consistent well with the X-ray structure of a model complex,[42] but it is rather long compared with 2.46 Å estimated from EXAFS analyses for the Fe···Fe distance of the actual intermediate **Q**.[12] We think 2.46 Å is unusually short for an $Fe_2(\mu\text{-}O)_2$ core with a carboxylato bridge. The structure of intermediate **Q** is thus of fundamental interest and subject of an ongoing controversy so that detailed X-ray structural analyses are necessary for a better understanding of the methane hydroxylation by sMMO. Although we utilized model complex **2** for a possible structure of intermediate **Q**, please note that our concerted mechanism needs an "unsaturated" iron-oxo species as an active center that affords a coordination site to methane.

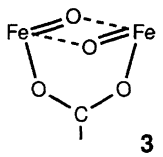


**3**

Chart 2.

Methane is activated on model complex **2** through the formation of the reactant complex, **2**($CH_4$), which involves interesting five-coordinate methane. The significant orbital interactions indicated in Scheme 2 result in the deformation of the coordinating methane; the three H–C–H angles of the methane moiety are decreased to 98.6, 99.3, and 99.7° (not indicated in the illustration) from the equivalent H–C–H angles of 109.5° in $T_d$-type free methane. The coordinating methane in the **2**($CH_4$) complex exhibits a $C_{3v}$-type structure that is expected for an $\eta^3$-binding mode **4** (Chart 3). Another important binding mode **5**, called $\eta^2$, is also possible to occur to our experience.[29] From a theoretical viewpoint we have proposed such methane-complexes in several conferences of the Chemical Society of Japan and others, but most bioinorganic chemists have been strongly against our proposal.

An H atom abstraction occurs in the **2**($CH_4$) complex via TS1, in which the optimized C–H and O–H bond distances

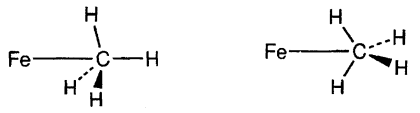


**4** **5**

Chart 3.

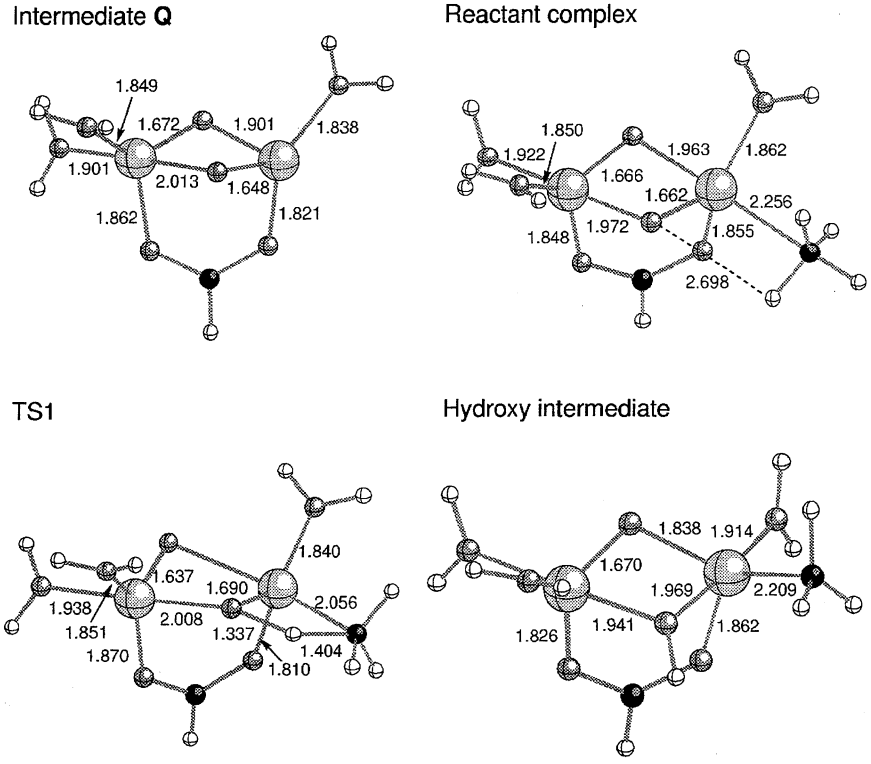


Fig. 3. Optimized geometries of a model of **Q** (**2**), the reactant complex, TS1, and the hydroxy intermediate.

are 1.404 and 1.337 Å, respectively. These distances are quite reasonable for the transition-state structure of a hydrogen abstraction. This four-centered structure is quite similar to the corresponding transition-state structure in the gas-phase methane hydroxylation by the $FeO^+$ complex.[22,29] We confirmed from high-level DFT calculations that the concerted reaction pathway for the H abstraction by the $FeO^+$ complex is lower than a radical pathway.[40] The structure of TS1 is different from that of the transition state for the direct H atom abstraction proposed by Siegbahn and Crabtree.[28] The reader may think that our mechanism cannot explain an observed kinetic isotope effect (KIE) of 4.2 for an H atom abstraction by sMMO,[43] but ours is consistent, because TS1 is responsible for the intramolecular H atom abstraction on the methane-complex. We can expect a small KIE for such an H atom abstraction or "migration". The diamond core is broken in TS1 since one of the optimized Fe–O distances is long: 2.34 Å.

The H atom abstraction leads to the formation of a reaction intermediate; we call it hydroxy intermediate. This intermediate corresponds to the important insertion species, $HO–Fe^+–CH_3$, in the gas-phase methane–methanol conversion by $FeO^+$. As mentioned above, Schröder and Schwarz[13a] have suggested that this intermediate should play a central role in the reaction between $FeO^+$ and methane. The generated hydroxy intermediate in Fig. 3 still includes a diamond core although it consists of oxo and hydroxo bridgings. The two Fe–O distances in the hydroxo bridging are nearly equal, in contrast to the oxo bridging in which one is 1.670 Å and another is 1.838 Å. The important initial step of our proposed reaction pathway is over with the formation of the important hydroxy intermediate.

The second half of the reaction begins by climbing over TS2, the energy barrier of which is small compared with that of TS1, as shown in Figs. 1 and 2. In Fig. 4 we show optimized geometries for TS2, the product complex, and the final complex from which methanol is already dissociated. TS2 which correctly connects the hydroxy intermediate and the product complex exhibits a three-centered structure responsible for an intramolecular methyl migration; the optimized Fe–C and O–C distances are 2.264 and 2.252 Å, respectively. Note that this structure still retains the diamond core.

The diamond core is not present in the product complex that involves methanol as a ligand; the oxygen atom of the methanol moiety is strongly bound to one of the iron centers. Interestingly, the optimized Fe–O distance (1.818 Å) is short, due to the limit of singlet calculations and to the charge-induced complexation, so that much energy is required for the liberation of the methanol from the product complex, especially in the singlet state. However, spin-unrestricted calculations afford a better, reasonable value for the liberation energy, as we saw in Fig. 2.

## Orbital Interaction Analyses

We carried out a fragment molecular orbital (FMO) analysis based on the extended Hückel method in order to have a better understanding of the H atom abstraction, the most important step for the conversion of methane to methanol. Figure 5 illustrates an FMO analysis of TS1, in which the d-block levels of the diiron complex are shown at the left, the HOMO of the deformed methane (coming from one of the threefold degenerate $t_2$) at the right, and the orbitals recon-

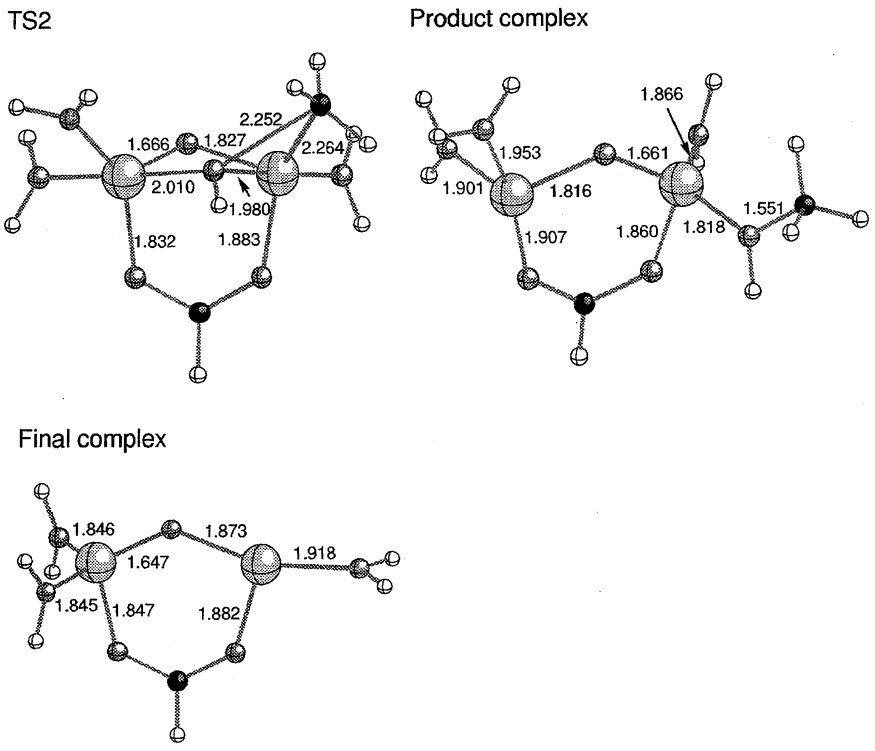


Fig. 4. Optimized geometries of TS2, the product complex, and the final complex from which methanol is dissociated.

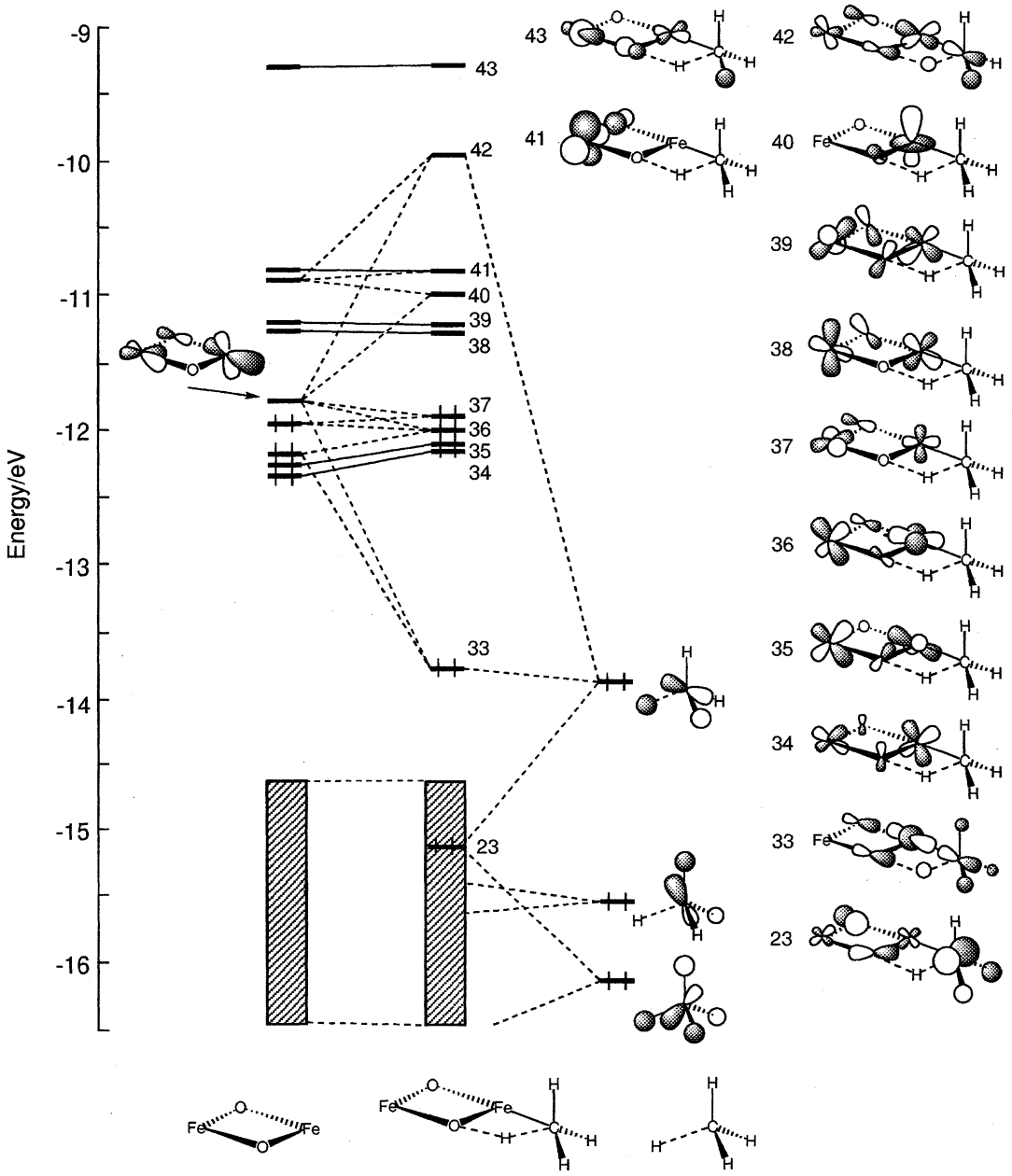


Fig. 5. Orbital interaction diagram for forming TS1, which connects the initial **Q**($CH_4$) complex and the hydroxy intermediate. The structure of TS1 is partitioned into **Q** and methane fragments.

structed from the two fragments at the center. Since the formal charge of the irons is +4, the lowest four d-block orbitals of the diiron complex at the left is occupied by eight electrons in the assumed singlet state. An important orbital interaction is that of the HOMO of the methane (at −13.8 eV) with one of the d-block orbitals of the diiron complex (at −11.8 eV) that points toward the coordinating methane. Since the orbital interactions indicated are a little complicated, due to contribution from other MOs, the methane HOMO splits into three, as indicated; the first one (#23) is pushed down to −15.2 eV, the second one (#33) is slightly destabilized, and the third one (#42) is significantly pushed up to −10.0 eV. The nonbonding d orbital at −11.8 eV at the left in Fig. 5 plays an important acceptor role in the interaction with the HOMO of the methane, because the high-lying #42 orbital resulting from the methane HOMO is clearly unfilled even in the high-spin nonet state in which all the eight orbitals of #34—#41 are singly occupied.

TS1 is responsible for a C–H bond cleavage and an O–H bond creation; thus it may be more informative to take a look at MOOP (molecular orbital overlap population)[44] analyses for the C–H and O–H bonds indicated in Fig. 6. These diagrams show graphically the contribution of various MOs to the overlap population. We show the bonding and antibonding interactions of the C–H and O–H bonds in the structure of TS1, in which the C–H distance is 1.404 Å and the O–H distance 1.337 Å. Bonding overlap populations are plotted to the right and antibonding ones to the left. The horizontal dot-

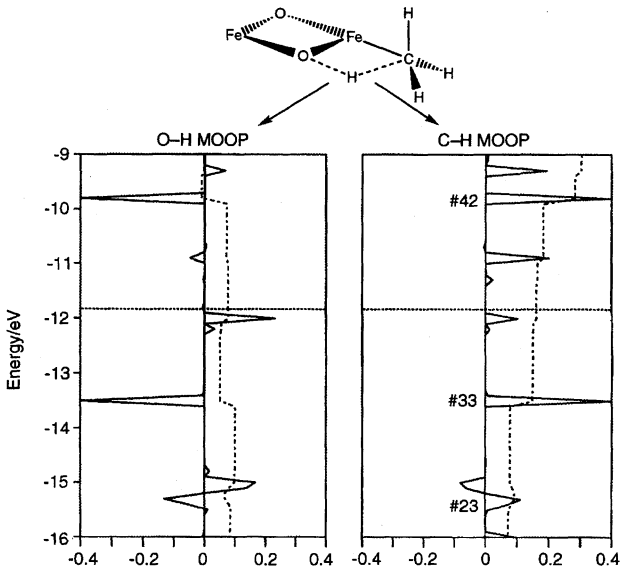


Fig. 6. MOOP (molecular orbital overlap population) analyses for the C–H and O–H bonds of TS1.

ted lines mark the HOMO, and the dashed lines running up indicate integrations up to the indicated energy of all bonding and antibonding contributions.

The #23, 33, and 42 orbitals are in-phase for the C–H bond and out-of-phase for the O–H bond, as shown in Fig. 6. However, as the dashed integrations indicate, there is substantial bonding for both the C–H and O–H bonds below the HOMO level. The bonding nature of the O–H bond is ascribed to other orbitals, as indicated at the left in Fig. 6.

## Discussion

Several mechanisms have been proposed for MMO-catalyzed hydroxylations; these invoke an intermediate substrate radical,[45,46] an additional substrate carbocation intermediate,[47] and a concerted oxygen insertion[48] into a substrate carbon–iron bond. Our mechanism proposed above differs from all of these mechanisms. One of the most important experimental results supporting a widely-believed radical mechanism for hydroxylations by cytochrome P450[27] as well as sMMO is kinetic isotope effect (KIE). Floss and Lipscomb reported a small KIE of 4.2 for hydrogen abstraction for ethane hydroxylation by sMMO.[43] In contrast to a concerted hydrocarbon hydroxylation mechanism (so-called oxenoid mechanism) proposed for P450 indicated in Scheme 3,[27] our two-step concerted mechanism is not inconsistent with the observed KIE because the proposed first transition state (TS1), which we showed in Scheme 1 and Fig. 3, is responsible for an H atom abstraction or migration from the substrate to the ferryl "oxygen". In such an H atom migration we can reasonably expect an occurrence of KIE.

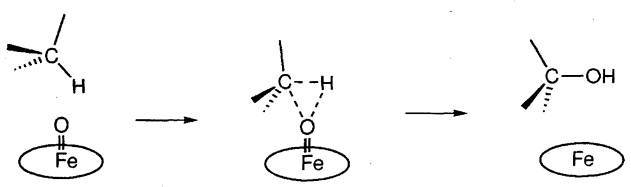


Scheme 3.

Another important experimental result that strongly supports a radical mechanism is the observed inversion of stereochemistry at a labeled carbon. Floss and Lipscomb et al.[43] and Lippard et al.[49] reported for sMMO-catalyzed hydroxylations that the product alcohol displayed 65—72% retention of stereochemistry at a labeled carbon for ethane substrate and 77% retention for butanes labeled at a primary carbon. In a previous paper,[24c] we suggested that inversion at a carbon center through "$D_{2d}$ deformation" of the substrate in an $\eta^2$-binding mode in a reactant complex can reasonably explain the observed inversion of stereochemistry, as indicated in Scheme 4. The activation barrier for such an inversion is significantly decreased in a reactant complex, in which the substrate is activated because of significant electron transfer discussed above.[24b] Since the HOMOs of alkanes are usually composed of C–H bonding orbitals, the coordinating alkane becomes "soft" for inversion at a carbon center if such electron transfer occurs. We believe that "$D_{2d}$ deformation" in an $\eta^2$-binding mode would lead to inversion of stereochemistry.

Let us next consider recent experiments on the regiochemical variations in reactions of methylcubane **6** (Chart 4) with *t*-BuO$^\bullet$ radical, cytochrome P450, and sMMO.[50] This study is very important in considering reaction mechanisms of the hydroxylations by these iron-based enzymes. A strong preference for cubyl hydrogen abstraction was observed in the reaction of **6** with *t*-BuO$^\bullet$. Thus, in a pure radical reaction of the *tertiary* cubyl hydrogen is preferred to the methyl hydrogen abstraction.

The regioselectivity observed in enzymatic hydroxylations of **6** considerably differs from that found in the alkoxyl radical abstraction. In the P450-catalyzed hydroxylations of **6**, the ratio of reactions at the cubyl positions to reaction at the methyl position is approximately one. Moreover, sMMO hydroxylase yielded products corresponding only to oxidation at the methyl position of **6**. These results cannot be reasonably explained by a simple radical mechanism that assumes direct H atom abstraction through a linear C–H–O array. Thus, the lack of reactivity at the cubyl C–H bonds would argue against the widely-accepted oxygen rebound mechanism, especially in the hydroxylations catalyzed by sMMO. On the basis of measured short "radical" lifetimes of ca. 100 fs and regiochemical variations in enzymatic hy-

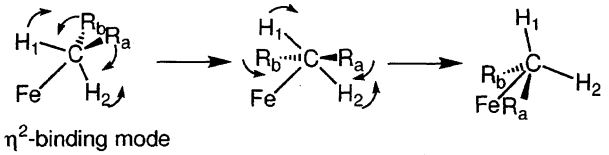


Scheme 4.

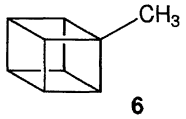


**6**

Chart 4.

droxylations, Lippard, Newcomb, and their collaborators[50,51] suggested possible triangular transition states of OCH in both the P450- and sMMO-catalyzed hydroxylations (like in Scheme 3). They rule out conventional hydrogen abstraction that involves a linear array of C–H–O. This model is slightly similar to that proposed by Shteinman[52] and by Shestakov and Shilov.[53] In their mechanism the carbon atom of $C_{3v}$-deformed hydrocarbons coordinates directly to the ferryl "oxygen". We agree with the proposed five-coordinate carbon species; however, our theoretical analyses[22,24—26,29] show that the interaction of $FeO\cdots CH_4$ is not attractive and that it does not lead to C–H bond activation.

We have proposed a two-step concerted mechanism including an initial reactant complex with an OFe–$CH_4$ bond, as shown in the illustration of Fig. 3. The reactant complex is not a transition state, but a local minimum on a potential energy surface. We think that both the $\eta^2$- mode and the $\eta^3$-binding mode indicated in Scheme 4 should play a role in the formation of the initial complex by which alkane C–H bonds are significantly activated (weakened) through the important orbital interactions, especially of type ① in Scheme 2. On the basis of our mechanism, we can reasonably explain the lack of reactivity at the cubyl C–H bonds of methylcubane **6** in the hydroxylation by sMMO. The cubyl carbon cannot coordinate to the ferryl "iron" active center of sMMO, due to steric hindrance, but the methyl carbon is accessible to the iron to form an initial reactant complex. As described above, hydrogen and alkyl migrations successively occur at the ferryl iron active center, leading to the conversion of alkane to alcohol. We think that the extremely short radical lifetimes estimated in sMMO-catalyzed hydroxylations[50] may be ascribed to the concerted alkyl migration via TS2 in Scheme 1. The time scale of such a migration is expected to be in the order of 100 fs.

## Summary and Conclusions

We propose a two-step concerted mechanism for the conversion of methane to methanol by intermediate **Q** of sMMO, the key species that exhibits direct reactivity toward methane. Our DFT computations demonstrate that the reaction pathway is essentially identical to that of the gas-phase methane hydroxylation by $FeO^+$, which proceeds through two kinds of transition states as indicated in Scheme 1. The first step is an intramolecular H atom migration or abstraction in the initially formed **Q**($CH_4$) complex which binds methane on a four-coordinate iron as a ligand. The structure of the transition state (TS1) responsible for the H atom abstraction exhibits a typical four-centered structure. The important intermediate thus generated includes OH and $CH_3$ groups directly coordinating to one of the iron centers of the dinuclear model of intermediate **Q**. This intermediate is converted into the product complex including methanol as a ligand via the second transition state (TS2) that is responsible for an intramolecular methyl migration. In our experience, the barrier heights for TS1 and TS2 significantly depend on the charge states of complex and the number of d electrons concerned with the reactions, and these two values determine the characteristics of the methane hydroxylation by iron-oxo species.[29,40] Therefore the energetics of the potential energy surfaces we presented in this paper can be improved from higher-level computations, but we believe that the general features of the reaction mechanism describe the important enzymatic function of sMMO reasonably well. Our study would also be useful for development of high-performance catalytic systems that are able to directly convert methane to methanol under mild conditions.

Table 1. Extended Hückel Parameters for Fe, O, C, and H Atoms; $H_{ii}$ Orbital Energy, $\zeta$ Slater Exponent

| Orbital | $H_{ii}$ (eV) | $\zeta_{i1}$ | $c_1$ | $\zeta_{i2}$ | $c_2$ |
|---|---|---|---|---|---|
| Fe4s | −9.1 | 1.9 | | | |
| Fe4p | −5.32 | 1.9 | | | |
| Fe3d | −12.6 | 5.35 | 0.5505 | 2.00 | 0.6260 |
| O2s | −32.3 | 2.275 | | | |
| O2p | −14.8 | 2.275 | | | |
| C2s | −21.4 | 1.625 | | | |
| C2p | −11.4 | 1.625 | | | |
| H1s | −13.6 | 1.3 | | | |

More than twenty years ago, Joseph Chatt stated at a certain international conference, "Methane will be the most popular ligand in coordination chemistry".[54] Here is a nice example for his statement.

## Appendix

Extended Hückel parameters used for iron, oxygen, carbon, and hydrogen atoms appear in Table 1.

Our study on methane monooxygenase was initiated at Cornell University as collaboration between one of the authors (K.Y.) and Professor Roald Hoffmann. It is a pleasure to acknowledge fruitful discussions with Professor Hoffmann, concerning methane activation. We are grateful to a Grant-in-Aid for Scientific Research on Priority Area "Molecular Biometallics" from the Ministry of Education, Science, Sports and Culture and to "Research for the Future" Program from the Japan Society for the Promotion of Science (JSPS-RFTF96P00206) for their support of this work. Computations were partly carried out at the Data Processing Center and the Supercomputer Laboratory of Institute of Chemical Research, Kyoto University.

### References

1) a) A. E. Shilov, "The Activation of Saturated Hydrocarbons by Transition Metal Complexes," Reidel, Dortrecht (1984); b) A. E. Shilov, "Metal Complexes in Biomimetic Chemical Reactions," CRC, Boca Raton (1996).

2) a) R. G. Bergman, *Science*, **223**, 902 (1984); b) B. A. Arndtsen, R. G. Bergman, T. A. Mobley, and T. H. Peterson, *Acc. Chem. Res.*, **28**, 154 (1995).

3) C. L. Hill, "Activation and Functionalization of Alkanes," Wiley, New York (1989).

4) J. A. Davies, P. L. Watson, J. F. Liebman, and A. Greenberg, "Selective Hydrocarbon Activation," VCH, New York (1990).

5) a) R. H. Crabtree, *Chem. Rev.*, **85**, 245 (1985); b) R. H.

Crabtree, *Chem. Rev.*, **95**, 987 (1995).

6) H. D. Gesser, N. R. Hunter, and C. B. Prakash, *Chem. Rev.*, **85**, 237 (1985).

7) J. H. Lunsford, *Angew. Chem., Int. Ed. Engl.*, **34**, 970 (1995).

8) J. J. Schneider, *Angew. Chem., Int. Ed. Engl.*, **35**, 1068 (1996).

9) C. Hall and R. N. Perutz, *Chem. Rev.*, **96**, 3125 (1996).

10) Recent reviews on methane monooxygenase: a) D. M. Kurtz, Jr., *J. Biol. Inorg. Chem.*, **2**, 159 (1997); b) B. J. Wallar and J. D. Lipscomb, *Chem. Rev.*, **96**, 2625 (1996); c) L. Que, Jr., and Y. Dong, *Acc. Chem. Res.*, **29**, 190 (1996); d) A. L. Feig and S. J. Lippard, *Chem. Rev.*, **94**, 759 (1994); e) J. D. Lipscomb, *Annu. Rev. Microbiol.*, **48**, 371 (1994); f) S. J. Lippard, *Angew. Chem., Int. Ed. Engl.*, **27**, 344 (1988).

11) S. -K. Lee, B. G. Fox, W. A. Froland, J. D. Lipscomb, and E. Münck, *J. Am. Chem. Soc.*, **115**, 6450 (1993).

12) L. Shu, J. C. Nesheim, K. Kauffmann, E. Münck, J. D. Lipscomb, and L. Que, Jr., *Science*, **275**, 515 (1997).

13) a) D. Schröder and H. Schwarz, *Angew. Chem., Int. Ed. Engl.*, **29**, 1433 (1990); b) H. Schwarz, *Angew. Chem., Int. Ed. Engl.*, **30**, 820 (1991); c) D. Schröder, A. Fiedler, J. Hrusák, and H. Schwarz, *J. Am. Chem. Soc.*, **114**, 1215 (1992); d) A. Fiedler, J. Hrusák, W. Koch, and H. Schwarz, *Chem. Phys. Lett.*, **211**, 242 (1993); e) A. Fiedler, D. Schröder, S. Shaik, and H. Schwarz, *J. Am. Chem. Soc.*, **116**, 10734 (1994); f) D. Schröder and H. Schwarz, *Angew. Chem., Int. Ed. Engl.*, **34**, 1973 (1995); g) R. Wesendrup, C. A. Schalley, D. Schröder, and H. Schwarz, *Chem. Eur. J.*, **1**, 608 (1995); h) S. Shaik, D. Danovich, A. Fiedler, D. Schröder, and H. Schwarz, *Helv. Chim. Acta*, **78**, 1393 (1995); i) M. F. Ryan, A. Fiedler, D. Schröder, and H. Schwarz, *J. Am. Chem. Soc.*, **117**, 2033 (1995); j) M. C. Holthausen, A. Fiedler, H. Schwarz, and W. Koch, *J. Phys. Chem.*, **100**, 6236 (1996); k) A. Fiedler, D. Schröder, H. Schwarz, B. L. Tjelta, and P. B. Armentrout, *J. Am. Chem. Soc.*, **118**, 5047 (1996).

14) a) N. Aristov and P. B. Armentrout, *J. Phys. Chem.*, **91**, 6178 (1987); b) R. H. Shultz, J. L. Elkind, and P. B. Armentrout, *J. Am. Chem. Soc.*, **110**, 411 (1988); c) L. S. Sunderlin and P. B. Armentrout, *J. Phys. Chem.*, **92**, 1209 (1988); d) R. Geoorgiadis and P. B. Armentrout, *J. Phys. Chem.*, **92**, 7060 (1988); e) P. B. Armentrout and J. L. Beauchamp, *Acc. Chem. Res.*, **22**, 315 (1989); f) P. A. M. van Koppen, J. Brodbelt-Lustig, M. T. Bowers, D. V. Dearden, J. L. Beauchamp, E. R. Fisher, and P. B. Armentrout, *J. Am. Chem. Soc.*, **112**, 5663 (1990); g) P. B. Armentrout, *Science*, **251**, 175 (1991); h) P. A. M. van Koppen, J. Brodbelt-Lustig, M. T. Bowers, D. V. Dearden, J. L. Beauchamp, E. R. Fisher, and P. B. Armentrout, *J. Am. Chem. Soc.*, **113**, 2359 (1991); i) D. E. Clemmer, N. Aristov, and P. B. Armentrout, *J. Phys. Chem.*, **97**, 544 (1993); j) Y.-M. Chen, D. E. Clemmer, and P. B. Armentrout, *J. Am. Chem. Soc.*, **116**, 7815 (1994); k) D. E. Clemmer, Y.-M. Chen, F. A. Kahn, and P. B. Armentrout, *J. Phys. Chem.*, **98**, 6522 (1994).

15) a) J.-Y. Saillard and R. Hoffmann, *J. Am. Chem. Soc.*, **106**, 2006 (1984); b) R. Hoffmann, *Rev. Mod. Phys.*, **60**, 601 (1988).

16) a) J. J. Low and W. A. Goddard, III, *J. Am. Chem. Soc.*, **106**, 8321 (1984); b) J. J. Low and W. A. Goddard, III, *J. Am. Chem. Soc.*, **108**, 6115 (1986); c) J. K. Perry, G. Ohanessian, and W. A. Goddard, III, *J. Phys. Chem.*, **97**, 5238 (1993).

17) a) M. R. A. Blomberg, U. Brandemark, and P. E. M. Siegbahn, *J. Am. Chem. Soc.*, **105**, 5557 (1983); b) M. R. A. Blomberg, P. E. M. Siegbahn, U. Nagashima, and J. Wennerberg, *J. Am. Chem. Soc.*, **113**, 424 (1991); c) M. R. A. Blomberg, P. E. M. Siegbahn, and M. Svensson, *J. Am. Chem. Soc.*, **114**, 6095 (1992); d) P. E. M. Siegbahn and M. R. A. Blomberg, *Organometallics*, **13**, 354 (1994); e) P. E. M. Siegbahn, *Organometallics*, **13**, 2833 (1994); f) P. E. M. Siegbahn, *J. Am. Chem. Soc.*, **118**, 1487 (1996); g) P. E. M. Siegbahn and R. H. Crabtree, *J. Am. Chem. Soc.*, **118**, 4442 (1996).

18) a) T. Ziegler, V. Tschinke, and A. D. Becke, *J. Am. Chem. Soc.*, **109**, 1351 (1987); b) T. Ziegler, V. Tschinke, L. Fan, and A. D. Becke, *J. Am. Chem. Soc.*, **111**, 9177 (1989); c) T. Ziegler, E. Folga, and A. Berces, *J. Am. Chem. Soc.*, **115**, 636 (1993).

19) a) N. Koga and K. Morokuma, *J. Phys. Chem.*, **94**, 5454 (1990); b) N. Koga and K. Morokuma, *J. Am. Chem. Soc.*, **115**, 6883 (1993); c) D. G. Musaev, N. Koga, and K. Morokuma, *J. Phys. Chem.*, **97**, 4064 (1993); d) D. G. Musaev, K. Morokuma, N. Koga, K. Ngyen, M. S. Gordon, and T. R. Cundari, *J. Phys. Chem.*, **97**, 11435 (1993); e) D. G. Musaev and K. Morokuma, *J. Chem. Phys.*, **101**, 10697 (1994); f) D. G. Musaev and K. Morokuma, *J. Phys. Chem.*, **100**, 11600 (1996).

20) a) S. Sakaki and M. Ieki, *J. Am. Chem. Soc.*, **113**, 5063 (1991); b) S. Sakaki and M. Ieki, *J. Am. Chem. Soc.*, **115**, 2373 (1993).

21) a) T. R. Cundari, *J. Am. Chem. Soc.*, **114**, 10557 (1992); b) T. R. Cundari and M. S. Gordon, *J. Am. Chem. Soc.*, **115**, 4210 (1993); c) T. R. Cundari, *J. Am. Chem. Soc.*, **116**, 340 (1994).

22) K. Yoshizawa, Y. Shiota, and T. Yamabe, *Chem. Eur. J.*, **3**, 1160 (1997).

23) a) K. Fukui, *J. Phys. Chem.*, **74**, 4161 (1970); b) K. Fukui, *Acc. Chem. Res.*, **14**, 363 (1981).

24) a) K. Yoshizawa and R. Hoffmann, *Inorg. Chem.*, **35**, 2409 (1996); b) K. Yoshizawa, T. Yamabe, and R. Hoffmann, *New J. Chem.*, **21**, 151 (1997); c) K. Yoshizawa, T. Ohta, T. Yamabe, and R. Hoffmann, *J. Am. Chem. Soc.*, **119**, 12311 (1997).

25) K. Yoshizawa, *J. Biol. Inorg. Chem.*, **3**, 318 (1998).

26) a) K. Yoshizawa, Y. Yokomichi, Y. Shiota, T. Ohta, and T. Yamabe, *Chem. Lett.*, **1997**, 537; b) K. Yoshizawa, T. Ohta, Y. Shiota, and T. Yamabe, *Chem. Lett.*, **1997**, 1213.

27) P. R. Ortiz de Montellano, "Cytochrome P450: Structure, Mechanism, and Biochemistry," 2nd ed, Plenum, New York (1995).

28) P. E. M. Siegbahn and R. H. Crabtree, *J. Am. Chem. Soc.*, **119**, 3103 (1997).

29) K. Yoshizawa, Y. Shiota, and T. Yamabe, *J. Am. Chem. Soc.*, **120**, 564 (1998).

30) M. J. Frisch, G. W. Trucks, H. B. Schlegel, P. M. W. Gill, B. G. Johnson, M. A. Robb, J. R. Cheeseman, T. A. Keith, G. A. Petersson, J. A. Montgomery, K. Raghavachari, M. A. Al-Laham, V. G. Zakrzewski, J. V. Ortiz, J. B. Foresman, J. Cioslowski, B. B. Stefanov, A. Nanayakkara, M. Challacombe, C. Y. Peng, P. Y. Ayala, W. Chen, M. W. Wong, J. L. Andres, E. S. Replogle, R. Gomperts, R. L. Martin, D. J. Fox, J. S. Binkley, D. J. Defrees, J. Baker, J. J. P. Stewart, M. Head-Gordon, C. Gonzalez, and J. A. Pople, "Gaussian 94," Gaussian Inc., Pittsburgh, PA (1995).

31) a) A. D. Becke, *Phys. Rev. A*, **38**, 3098 (1988); b) A. D. Becke, *J. Chem. Phys.*, **98**, 5648 (1993).

32) C. Lee, W. Yang, and R. G. Parr, *Phys. Rev. B*, **37**, 785 (1988).

33) S. H. Vosco, L. Wilk, and M. Nusair, *Can. J. Phys.*, **58**, 1200 (1980).

34) P. J. Hay and W. R. Wadt, *J. Chem. Phys.*, **82**, 299 (1985).

35) T. H. Dunning, Jr., and P. J. Hay, "Modern Theoretical Chemistry," ed by H. F. Schaefer, III, Plenum, New York (1976), p. 1.

36) M. N. Glukhovtsev, R. D. Bach, and C. J. Nagel, *J. Phys. Chem. A*, **101**, 316 (1997).

37) Our computations can be improved by using higher-level

multiconfigurational methods, but we believe that the essential features of the energetics and the reaction species along the reaction pathway are described reasonably well with the present DFT method.

38) a) R. Hoffmann, *J. Chem. Phys.*, **39**, 1397 (1963); b) R. Hoffmann and W. N. Lipscomb, *J. Chem. Phys.*, **36**, 2179 (1962); **37**, 2872 (1962).

39) G. A. Landrum, "YAeHMOP : Yet Another extended Hückel Molecular Orbital Package," version 2.0, Cornell University, Ithaca, New York (1997).

40) K. Yoshizawa, Y. Shiota, and T. Yamabe, *Organometallics*, **17**, 2825 (1998).

41) J.-Y. Saillard and R. Hoffmann, *J. Am. Chem. Soc.*, **106**, 2006 (1984).

42) L. Que, Jr., *J. Chem. Soc., Dalton Trans.*, **1997**, 3933.

43) N. D. Priestley, H. G. Floss, W. A. Froland, J. D. Lipscomb, P. G. Williams, and H. Morimoto, *J. Am. Chem. Soc.*, **114**, 7651 (1992).

44) MOOP was introduced by D. M. Prosperio and C. Mealli in CACAO (a package of programs for extended Hückel molecular orbital analysis).

45) a) B. G. Fox, W. A. Froland, J. Dege, and J. D. Lipscomb, *J. Biol. Chem.*, **264**, 10023 (1989); b) B. G. Fox, J. G. Borneman, L. P. Wackett, and J. D. Lipscomb, *Biochemistry*, **29**, 6419 (1990).

46) a) J. Green and H. Dalton, *J. Biol. Chem.*, **264**, 17698 (1989); b) N. Deighton, I. D. Podmore, M. C. R. Symons, P. C. Wilkins, and H. Dalton, *J. Chem. Soc., Chem. Commun.*, **1991**, 1086.

47) F. Ruzicka, D.-S. Huang, M. I. Donnelly, and P. A. Frey, *Biochemistry*, **29**, 1696 (1990).

48) a) D. H. R. Barton, E. Csuhai, D. Doller, N. Ozbalik, and G. Balavoine, *Proc. Natl. Acad. Sci. U.S.A.*, **87**, 3401 (1990); b) D. H. R. Barton, S. D. Béviere, W. Chavasiri, E. Csuhai, D. Doller, and W.-G. Liu, *J. Am. Chem. Soc.*, **114**, 2147 (1992).

49) A. M. Valentine, B. Wilkinson, K. E. Liu, S. Komar-Panicucci, N. D. Priestley, P. G. Williams, H. Morimoto, H. G. Floss, and S. J. Lippard, *J. Am. Chem. Soc.*, **119**, 1818 (1997).

50) S. Y. Choi, P. E. Eaton, P. F. Hollenberg, K. E. Liu, S. J. Lippard, M. Newcomb, D. A. Putt, S. P. Upadhyaya, and Y. Xiong, *J. Am. Chem. Soc.*, **118**, 6547 (1996).

51) M. Newcomb, M. H. Le Tadic-Biadatti, D. L. Chestney, E. S. Roberts, and P. F. Hollenberg, *J. Am. Chem. Soc.*, **117**, 12085 (1995).

52) A. A. Shteinman, *Izv. Akad. Nauk Ser. Khim.*, **1995**, 1011; *Russ. Chem. Bull.*, **44**, 975 (1995).

53) A. F. Shestakov and A. E. Shilov, *Zh. Obshch. Khim.*, **65**, 60 (1995); *J. Mol. Cat. A*, **105**, 1 (1996).

54) Statement at the 17th International Conference on Coordination Chemistry, Hamburg, 1976; see also Chapter 2 of Ref. 1b.